ORIGINAL PAPER

Surg. Gastroenterol. Oncol. 2026;31(2 Suppl):S43-S54 DOI: 10.21614/sgo-767

Study of the Cytotoxic Effects of Zinc Oxide Nanoparticles (ZnO-NPs) on PC-3 Cancer Cell Line

Maysam Kareem Hassan, Rasha Salih Nuhair*

***Corresponding author:**
Rasha Salih Nuhair, MD
University of Thi-Qar
College of science, Thi-Qar, Iraq
E-mail: rasha.n-bio@sci.utq.edu.iq

University of Thi-Qar, College of science, Thi-Qar, Iraq

ABSTRACT

Background: The present study was aimed at the green synthesis and characterization of zinc oxide nanoparticles (ZnO-NPs) derived from Aspergillus niger, and the evaluation of their cytotoxic effects on the prostate cancer cell line (PC-3).
Method: The synthesized NPs were characterized by various analytical techniques, including ultraviolet-visible spectroscopy (UV-Vis), atomic force microscopy (AFM), Energy Dispersive X-ray (EDX) and Field Emission Scanning Electron Microscopy(FE-SEM). Furthermore, the cytotoxic effects on PC-3 cells were investigated using high- content screening and caspase - 8 and caspase -9 activity assays.
Result: The results demonstrated the ability of the ZnO-NPs to reduce cancer cell viability in a dose-dependent manner within IC50 of 9.712 µg/mL in comparison to an IC50 of 170. 2 µg/mL for the normal cell line (HdFn). A significant increase in caspase - 8 and caspase - 9 activity was also observed when PC-3 cells were treated with ZnO-NPs (200 µg/mL). Furthermore, increased mitochondrial membrane permeability, cytochrome c levels, and nuclear intensity were observed with ZnO-NPs (200µg/mL) compared with the untreated control.
Conclusion: These findings show that ZnO-NPs synthesized from fungal extract possess potent cytotoxic effects on human prostate cancer cell lines. as demonstrated by high-content screening and caspase-8 and 9 activity assays.
Keywords: prostate cancer, PC-3, ZnO-NPs , high- content screening, cytotoxic effect

INTRODUCTION

Cancer is a significant burden on human health and represents the second leading cause of death worldwide. According to the World Health Organization (WHO), cancer - related deaths are more prevalent in developed countries than in developing ones (1). Cancer treatment remains challenging and over the past decade, it has become a leading cause of mortality in developing nations. Therefore, cancer is a critical problem impacting human societies globally. At the tissue level, cancer encompasses a variety of diseases , diagnosing it is the primary challenge, followed by the efficacy of treatment (2). Prostate cancer (PCa) is a leading causes of illness and death in both developing and under-developed nations. (3). PCa is a major contributor to cancer incidence in males globally, including in the United States, where it was expected to account for 191,930 new cases and 33,330 deaths in 2020 (4).

Received: 12.03.2026
Accepted: 17.06.2026

Copyright © Celsius Publishing House
www.sgo-iasgo.com

Cancer has developed into one of the most metastatic diseases , it lack a definitive cure and frequently resists chemotherapy and radiation (5). Therefore, there is an unmet need for more advanced chemo-preventive substances that can stop or slow the development of cancer (6). Anticancer drug development research aims to identify natural and synthetic compounds that can be used in treatment to increase effectiveness while reducing toxicity. In recent years, researchers have focused on the topic of nanotechnology, which has made significant great in producing pharmaceuticals for cancer treatment. As drug carriers, nanoparticles (NPs) deliver drugs directly to the tumor site while preserving healthy tissue, offering numerous advantages over traditional chemotherapeutic drugs (7,8). In recent years, researchers have focused on nanotechnology, which has made significant progress in producing pharmaceuticals for cancer treatment. As drug carriers, nanoparticles (NPs) deliver the drug directly to the tumor site while preserving healthy tissue. In this context, green nanotechnology is a developing field for producing environmentally friendly materials that contribute to sustainable development (9,10). Biosynthetic techniques eliminate the use of harmful chemicals, reduce high energy demand, and avoid the need for high pressures and temperatures. This process involves the use of living organisms such as bacteria, fungi, algae, yeasts, molds, viruses, and mostly plants (11,12).

These organisms act as miniature nano-factories where the enzymes, proteins or biomolecules they release facilitate the selective reduction metal ions into their respective metal or metal oxide NPs (13). Fungi produced enzymes that can be employed to synthesize nanoparticles of defined size and shape; Unlike other microorganisms, fungi can endure high agitation and flow pressure effectively (14). The endopytic fungus *Aspergillus niger* has been utilized for the production of zinc oxide nanoparticles (15). The exploration of semiconductor nanoparticles including ZnO-NPs has emerged as a key area of scientific research, due to their essential role in advanced technological applications. As semiconductor material are reduced to the nanoscale, their chemical and physical properties. undergo substantial alteration, resulting in unique features related with large surface area and quantum size effects. These changes significantly impact the optical properties of the semiconductor's such as its refractive index and absorption coefficient and conductivity (16)

The use of ZnO-NPs in cancer treatment has attracted significant interest from researchers, with numerous studies show casing their anticancer properties (17). The present study aimed at the synthesis and characterization of ZnO-NPs by A. niger to be applied for cytotoxic and anticancer activities.

MATERIALS AND METHODS

Preparation and Standardization of Aspergillus niger Inoculum

To ensure precision and reproducibility in antifungal susceptibility testing, Aspergillus niger was previously identified by PCR and obtained from the Fungi Laboratory at the Centre for Environment, Water, and Renewable Energy (Ministry of Higher Education and Scientific Research, Iraq) was utilized. The fungal strain was sub-cultured on Potato Dextrose Agar (PDA) supplemented with 250 mg/L of chloramphenicol to inhibit bacterial contamination and incubated at 28°C for five days. For inoculum preparation, fungal colonies grown for 5–7 days were transferred into sterile tubes containing 5–10 mL of sterile distilled water or saline, following the methodology described by (18). The resulting mixture, consisting of conidia and small hyphal fragments, was allowed to settle to remove heavier debris. Subsequently, the suspension was standardized to a final concentration of 1–5 × 10^3 cells/mL by direct microscopic counting using a haemocytometer, in accordance with the CLSI M38-A2 guidelines.

Preparation of Aspergillus niger extract

To prepare the fungal biomass for NPs biosynthesis, the A. niger was cultured aerobically of Potato Dextrose Broth media in 1000 mL. The broth was supplemented with chloramphenicol (250 mg/L) as an antibacterial agent and the pH was adjusted to 6.5. The flasks containing above media were incubated at 28 ºC for 14-21 days in shaking incubator then agitated at 150 rpm. After the incubation, fungal mycelia were separated from broth by filtration with sterile Whatmann filter paper No. 1 and the settled mycelia were washed with sterile distilled water followed by a washing step with deionised distilled water to remove any medium components from the biomass that might interact with metal ions. 20 grams of fungal biomass were weighted and inoculated in 200 mL deionized water for 72 hours in 500 mL Erlenmeyer flask and agitated as earlier described. After the incubation, the cell filtrate was separated by filtration through Watmann filter paper No. 1 the watery filtrate was dried in a hot air oven at

55-60°C for a whole night before being used in the biogenesis of nanoparticles (19).

Biosynthesis of the Zinc Oxide Nanoparticle

The biogenic production of ZnO-NPs was conducted using a modified methodology (20,21). 10% fungus extract solution (15 mL) was added conical flask containing 1000 mL of 0.06 M into zinc sulphate solution, when the temperature attained 60 °C on a magnetic stirrer and was maintained for approximately 2 hours. The addition sodium hydroxide (0.1M) subsequently neutralised the mixture's acidity. Under intense agitation, the stirring was sustained for 12 hours. Following that, the mixture was kept at 60 °C for the entire night in order to make a creamy paste. This paste was collected and washed several times with a solution of distilled water: Ethanol (3:1). Following its transfer to a ceramic crucible, the paste was baked for 24 hours at 50°C in an electric oven before being ground into powder using an agate mortar. Finally, resultant white powder is kept for characterisation in an airtight container.

Characterization of ZnO-NPs

UV-Vis Spectroscopy

The absorbance spectra of nanoparticle solution were analysed using UV-VIS double- beam spectrophotometer (Shimadzu, Japan). All spectra were collected in a quartz cell with a 1 cm optical path length at ambient temperature, using as a deionised distilled water as a control. The absorbance was measured using the wavelength range of 200 – 800 nm, and concentrated samples were diluted at a ratio of 1:10 (22).

FE-SEM Analysis

The surface morphology was analysed using a field emission scanning electron microscope FE-SEM (Bruker, USA) (23). Samples were prepared by applying seven drops of the nanoparticles suspension onto a glass slide and allowing them to dry.

AFM Analysis

The surface morphology of the nanoparticles was examined using an Atomic Force Microscope (Perkin Elme, USA) in contact mode and under normal atmospheric conditions. A solution of the nanoparticles was applied as drops on a glass slide (1×2 cm) and allowed to dry, the slide was placed on the AFM sample stage, and the analysis was conducted according to the standard procedure (24).

EDX Analysis

Elemental composition was determined using an Energy Dispersive X-ray (EDX) system (Zeiss, Germany) equipped with an Oxford Instruments INCA 350 detector, featuring a 10 mm^2 area and a resolution of 133 eV at manganese (Mn) (25).

Biological Activity

MTT assays, High- content screening (HCS) and Caspase- 8 and Caspase-9 assays were performed at the Natural Product Research and Drug Discovery Centre, located in the Department of Pharmacology at the Faculty of Medicine, University of Malaya, Kuala Lumpur, Malaysia.

Cytotoxic Effect of ZnO-NPs on PC-3 Cancer Cell Line

MTT Assay

The cytotoxic effects of ZnO-NPs were evaluated on both the PC-3 cancer cell line and the HdFn normal fibroblast cell line (used as a control) using an MTT assay (Bio-Rad, USA). Cells were maintained and cultured according to established protocols. Briefly, cells were grown in culture flasks until a confluent monolayer was achieved. The cells were then detached using 3 mL of trypsin-versene solution and incubated at 37°C for 1–2 minutes. Subsequently, 15 mL of RPMI medium was added to neutralize the trypsin, and cell density was determined using a hemocytometer. PC-3 and HdFn cells were seeded in 96-well microtiter plates at a density of 1 x 10^4 cells/mL in a final volume of 200 µL per well and incubated at 37°C for 24 hours. Following this, the medium was replaced with fresh medium containing varying concentrations of ZnO-NPs (25–400 µg/mL). All experimental treatments and control groups were performed in triplicates. After 24 hours of exposure to the nanoparticles, 10 µL of MTT solution was added to each well, and the plates were incubated for 4 hours at 37 °C in a 5% CO2 atmosphere. Finally, the medium was removed, 100 µL of the kit solubilization solution was added, and the plates were incubated for 5 minutes. The formation of formazan was quantified by measuring absorbance at 570 nm using an ELISA microplate reader (26).

High-Content Screening Assay

The cytotoxicity of ZnO-NPs on PC-3 cells was evaluated using the Thermo Scientific Cellomics multiparameter cytotoxicity kit. Cells were treated with varying concentrations of ZnO-NPs (25, 50, 100, and

200 µg/mL), and all experimental procedures were performed in triplicates for each concentration to ensure statistical reliability. To detect cellular changes, primary antibodies such as Cytochrome C and fluorescent dyes including DyLight™ 649 and Hoechst stain were utilized to assess parameters such as cell membrane permeability, mitochondrial membrane potential (MMP), and cytochrome c release. The samples were subsequently analyzed using an ArrayScan XTI computerized imaging microscope (Thermo-Scientific) equipped with a Zeiss 40 × 0.75 NA objective lens to quantify the fluorescence intensity in treated cells compared to the untreated cell (27).

Caspase-8 and Caspase-9 Activity Assays

The activity of Caspase-8 and Caspase-9 was measured to detect the induction of apoptosis using the Caspase-Glo® assay (Promega, USA) according to the manufacturer's protocols. PC-3 cells were seeded at a density of 1 x 10^4 cells/mL in 96-well plates and exposed to different concentrations of ZnO-NPs (50, 100, and 200 µg/mL) for 24 hours, with all treatments conducted in triplicates. Following the incubation period, 100 m L of Caspase-Glo 8 and 9 reagents were added to each well, and the plates were incubated at room temperature for 30 minutes. The assay mechanism relies on the cleavage of an aminoluciferin-labeled synthetic tetrapeptide substrate by the active enzymes within the apoptotic cells, resulting in luminescence that was measured using a microplate reader (28).

Statistics

A one-way analysis of variance ANOVA (Tukey Test) was performed to test whether group variance was significant or not, statistical significance was defined as *p ≤ 0.05 and **p ≤ 0.01. All experiments were performed in triplicates and data were expressed as mean± standard deviation and statistical significances were carried out using Graph Pad Prism version 8 (Graph Pad Software Inc., La Jolla, Co).

RESULTS

Biosynthesis of zinc oxide nanoparticles (ZnO-NPs)

Fig. 1 shows the synthesis of ZnO-NPs during the formation of a white precipitate of the end of the reaction using a reduction of aqueous zinc sulphate solution with cell-free filtrates of fungus A.niger at 28°C temperature. The ability of A. niger on synthesis of nanoparticles from zinc sulfate ZnSO4.7H2O and reduced the particles from micro to nano size were depended on the enzymes and the metabolic pathways that needed from fungal isolate. The precipitate was dried and used to study various charactererstic including UV-VIs, AFM, EDX and FE-SEM.

Characterization of Synthesized Zinc Oxide Nanoparticles

UV - Visible spectroscopy analysis of ZnO-NPs

UV–visible spectroscopy is a essential technique for confirming the synthesis of zinc nanoparticles (ZnONPs). The absorbance of the ZnO-NPs was measured, and the results illustrated in *fig. 2*. *Table 1* displays the absorbance values at various wavelength. the ZnONPs showed a maximum absorbance value of 3.763 at wavelength 233 and a minimum absorbance value of 0.3 at 301 nm.

FE-SEM Analysis of ZnO - NPs

The morphology of zinc oxide nanoparticles (ZnO - NPs) was analyzed using a field emission scanning

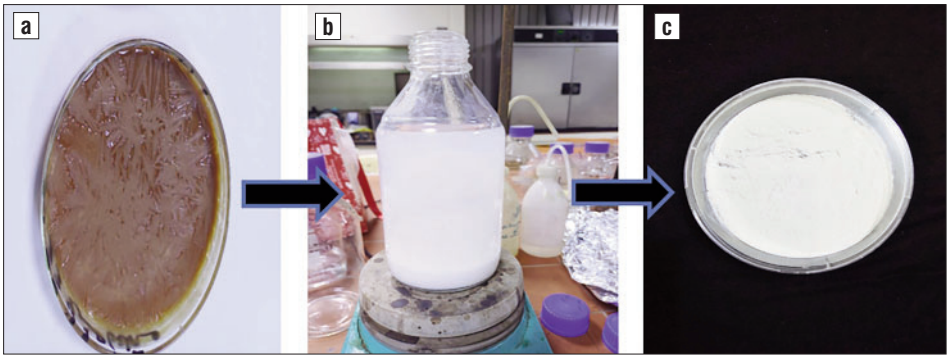


Figure 1 - Synthesis steps ZnO- NPs: (a) Dried A. niger extract, (b) Mixture reaction (ZnSO4.7H2O Salt with extract) after adding NaOH and (c) ZnO-NPs

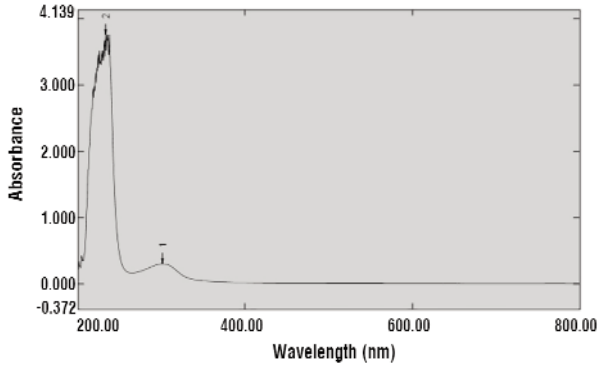


Figure 2 - UV- Visible spectral analysis of ZnO-NPs

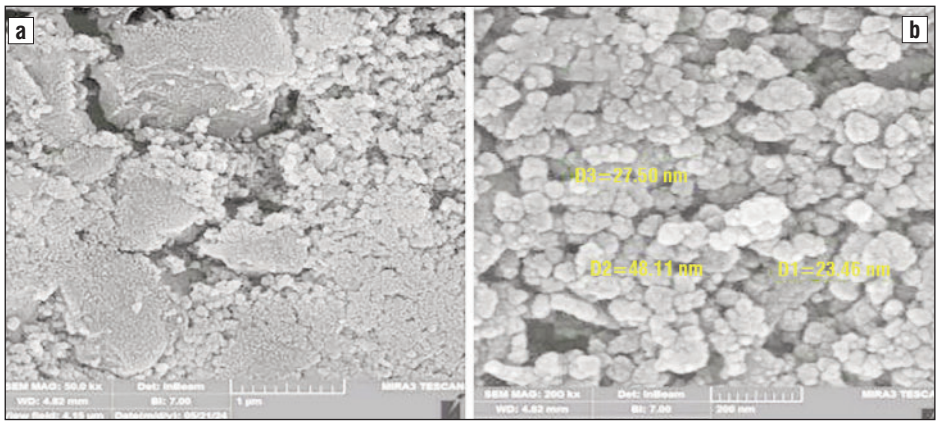
Table 1 - UV-Visible spectral analysis of ZnO- NPs

Absorbance	Wavelength	NO
0.310	301.00	1
3.763	233.00	2

Table 2 - Elemental analysis of ZnO-NPs by EDX

No	Element	W%	A%
1	Carbon	7.43	11.52
2	Oxygen	63.80	74.20
3	Sulfur	20.63	11.97
4	Zinc	8.14	2.32
	100.00	100.00	

Figure 3 - Field emission scanning electron microscopy (FE-SEM) morphology of the zinc oxide nanoparticles (ZnO-NPs) at (a) MAG 50.0 KX and (b) MAG 200 KX



electron microscope (FE-SEM), and the result s are shown in *fig. 3*. The ZnO-NPs appearance spherical shape with a diameter ranging from 23.46 to 48.1 nm, and have a relatively uniform morphology.

EDX Analysis of ZnO -NPs

The EDX spectra of the synthesized zinc nanoparticles confirm their purity . indicating the presence of essential zinc and oxygen phases, as shown in *table 2*. The atomic percentage of zinc was 02.32%, with a weight percentage of 8.14%. In contrast, oxygen atomic weight was 74.20%, while its weight percentage was 63.80%. Additionally, the presence of minor constituents in the ZnO- NPs s can be attributed to the A. niger extract , as illustrated in *fig. 4*. The EDX spectra exhibited three peaks for at approximately 1 keV, 8.6 keV, and 9.6 keV, along with a single peak for oxygen at around 0.5 keV, which are characteristic features of ZnO nanoparticles.

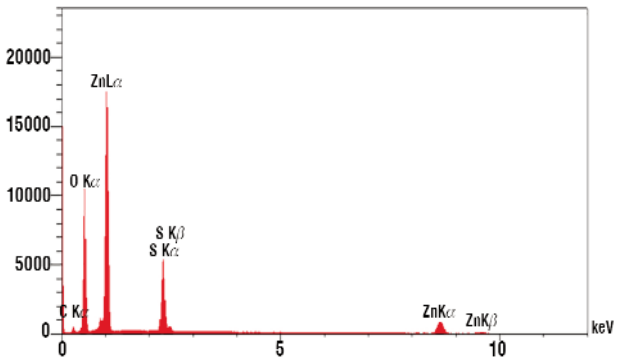


Figure 4 - Spectrum of elemental analysis of ZnO-NPs by EDX

AFM Analysis of ZnO- NPs

Atomic force microscopy (AFM) was utilized to evaluated the surface morphology of ZnO-NPs synthesized with A. niger filtrate. Both two dimensional and three-dimensional AFM images were obtained in non-contact mode as shown in *fig. 5*. These results agreed with which reported that the resulting morphological characteristics of the zinc nanoparticles exhibited uniform particles with an average size ranging from 20 to 100 nm.

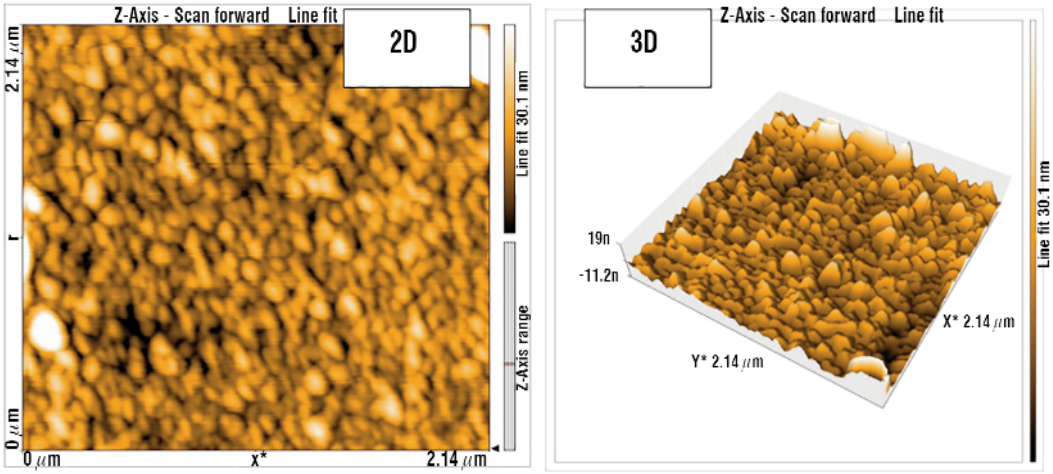


Figure 5 - Three and two dimensional image of ZnO -NPs by AFM

Cytotoxic Effects of the ZnO-NPs Using MTT Assay

The results of these parameters indicated that cell viability was decreased in PC-3 cell viability percentage noted by 400 µg/ml (44.48±1.34) while 25 µg/ml represented the uppermost cell viability to be reached (88.61± 0.86). The IC50 rate of 9.712 µg/ml of ZnO NPs cytotoxicity effect on cancer cells while the IC50 of 170.2 µg/ml on normal cell HdFn as shown in *table 3* and *fig. 6*.

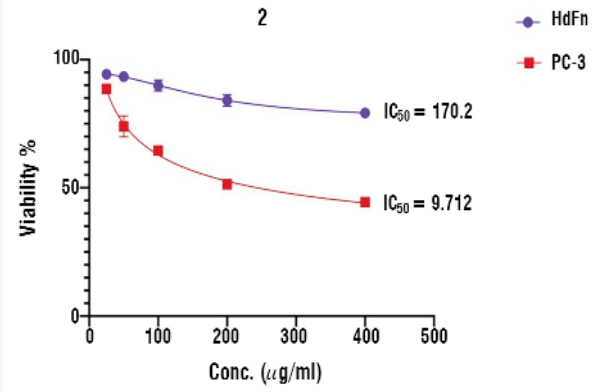


Figure 6 - Cytotoxicity effect of of ZnO - NPs on HdFn and PC-3 cell lines

Cytotoxic Effects of ZnO-NPs on PC-3 Cells Using HCS

The cytotoxicity of ZnO-NPs in PC-3 cells for 24 h was evaluated by HCS. Four ZnO-NPs concentrations (25,50,100 and 200 µg/mL) were used to detect changes in PC-3 cell viability, nuclear intensity, membrane permeability, mitochondrial membrane potential, and cytochrome C. The significant alterations in such parameters were investigated in comparison with untreated cells as control results in *fig. 7*, hardly confirm MTT results, in which the viability of PC-3 decreased by increasing the concentration of ZnO-NPs compared with untreated cells. No significant alteration in viability was detected in cells treated with 25 and

Table 3 - The cytotoxic effect of ZnO-NPs on HdFn and PC-3 cell lines

Concentration µg / ml	Mean viability(%) ± SD	
	HdFn	PC-3
400	79.20±1.57	44.48±1.34
200	84.14±2.23	51.35±1.44
100	89.89±2.18	64.50±1.77
50	93.40±0.53	73.99±4.16
25	94.25±1.14	88.61±0.86

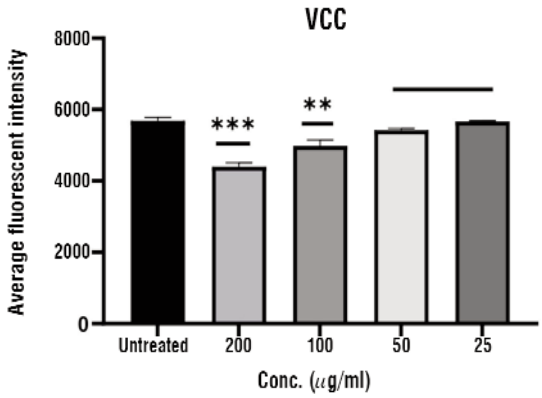


Figure 7 - Cytotoxicity effect of ZnO-NPs on viable cell count of PC-3 cell line on multipara system High Content screening at 37˚C. Data expressed as (mean± SD) **,,* p ≤ 0.05, SD: Standard Deviation, (n = 3)**

Table 4 - Cytotoxic effects of ZnO- NPs on cellular parameters by HCS

Concentration (µg/ml)	HCS Parameters (Mean ± SD)				
	VCC	TNI	CMP	MMP	CC
Untreated	5688 ± 94.75 [a]	458 ± 4.24 [a]	237 ± 5.65 [a]	768 ± 4.24 [a]	460 ± 9.89 [a]
200	4401 ± 107.48 [b]	681.5 ± 9.19 [b]	257 ± 8.48 [a]	557.5 ± 6.36 [b]	679 ± 5.65 [b]
100	4983 ± 164.04 [c]	566 ± 4.24 [c]	232.5 ± 12.02 [a]	646 ± 18.3 [c]	578.5 ± 4.94 [c]
50	5421.5 ± 48.79 [a]	474.5 ± 9.19 [a]	232.5 ± 0.70 [a]	765 ± 5.65 [a]	456 ± 2.82 [a]
25	5667 ± 22.62 [a]	464.5 ± 14.84 [a]	229 ± 9.89 [a]	770.5 ± 9.19 [a]	455 ± 9.89 [a]

VCC: Viable Cell Count; TNI: Total Nuclear Intensity; MMP: Mitochondrial MembranePotential; CMP: Cell Membrane Permeability; CC: Cytochrome C. Letters (a, b and c) are significant at $p \leq 0.05$, (n = 3)

50 µg/mL However, the viability of PC-3 cells was significantly decreased at 200 µg/ mL (4401 ±107.48) compared to the untreated cells as seen in *table 4*.

Similarly, the total nuclear intensity (TNI) increased significantly at 200 µg/mL-1 (681.5 ± 9.19) and 100 µg/ml (566 ± 4.24), indicating enhanced nuclear damag. In contrast lower ZnO-NPs concentrations (25 and 50 µg/ml) showed no significant difference in nuclear intensity, compared to the untreated control *fig. 8*.

On the other hand, no significant differences were recorded to cell membrane permeability between untreated cell and ZnO-NPs treatment at all concentrations *fig. 9*.

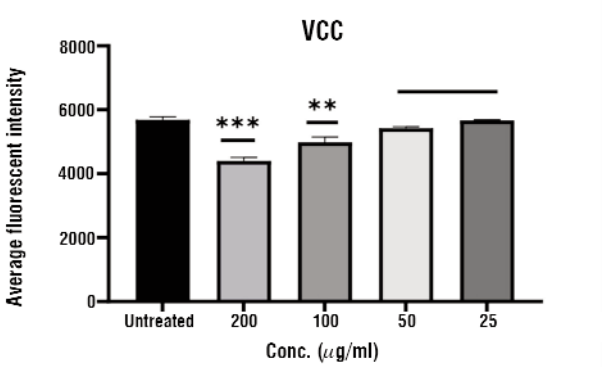


Figure 8 - Cytotoxicity effect of ZnO -NPs on the nuclear intensity of PC-3 cell line on multipara system High Content Screening at 37˚C. Data expressed as (mean ± SD) *,**** $p \leq 0.05$, SD: Standard Deviation.**

RESULTS

Figure 10 showed a dose-dependent decline in MMP intensity by increasing ZnO-NPs concentration with (557.5 ± 6.36) at 200 µg/ ml, comparing to untreated control. Regarding cell compactness (CC), elevated values were detected at 200 µg/ml (679 ± 5.65) and 100 µg/ml (578.5 ± 4.94), indicating alterations in cellular structure, possibly due to apoptotic progression. In contrast, lower concentrations (25 and 50 µg/ml) showed no significant differences compared to the untreated cell in most parameters *fig. 11*.

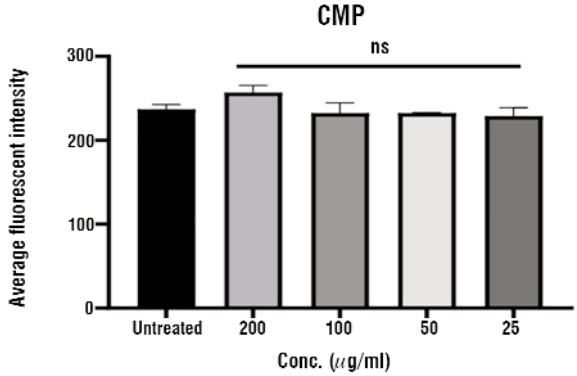


Figure 9 - Cytotoxicity effect of ZnO -NPs on cell membrane permeability of PC-3 cell line on multipara system High Content Screening at 37˚C. Data expressed as (mean ± SD), SD: Standard Deviation. (n = 3),NS: non-significant.

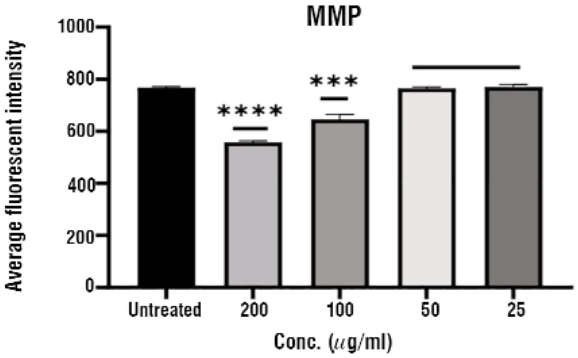


Figure 10 - Cytotoxicity effect of ZnO- NPs on mitochondrial membrane permeability of PC-3 cell line on multipara system High Content Screening at 37˚C. Data expressed as (mean ± SD) *,,**** $p \leq 0.05$, SD: Standard Deviation. (n = 3). .**

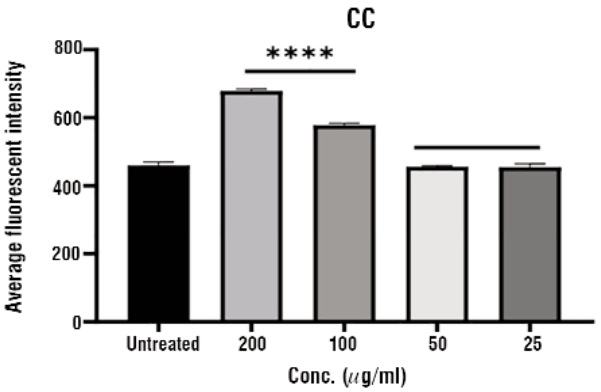


Figure 11 - Cytotoxicity effect of ZnO -NPs on cytochrome C of PC-3 cell line on multipara system High Content Screening at 37˚C. Data expressed as (mean ± SD)* *,* *** p ≤ 0.05, SD: Standard Deviation. (n = 3).**

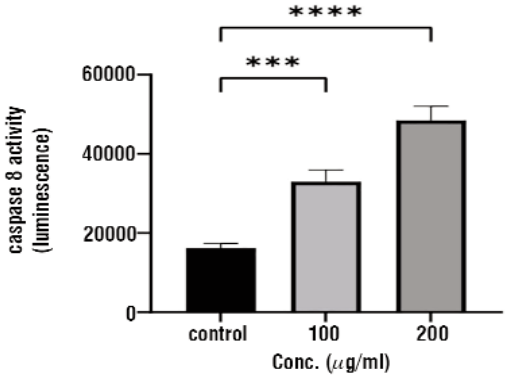


Figure 12 - Activation of caspase -8 activity by ZnO-NPs. Results were increase compared with untreated cell. Data represents mean ± SD of three independently repeated experiments

Caspase-8 and Caspase-9 Induction

Caspase-8 and caspase-9 are cysteine protease initiators that regulate the activation of series of effector caspases and mediate programmed cell death. The induction and activity levels of caspase 8 and 9 were detected in PC-3cells treated with ZnO-NPs. As shown in *fig. 12* a significantly dose dependent increasing in caspase 8 activity was detected in PC-3 treated with ZnO-NPs at concentrations 100 µg/ml (32972 ± 2971.75) and 200 µg/ml (48466 ± 3580.018) compared with the untreated cell *table 5*.

On the other hand, the activity of caspase-9 was also determined by examining PC-3 cells treated with increasing concentrations of ZnO-NPs for 24 hrs. Results in *fig. 13*, illustrates that the activity of caspase -9 significantly increased at ZnO-NPs concentration 200 µg/ ml with (27903 ± 3065.134) increase, comparing with untreated cells after 24-hour *table 6*.

Table 5 - Comparison of caspase-8 activity in luminescence (Mean± SD) in PC3 treated cells with 50, 100 and 200 µg/ml ZnO-NPs for 24 hrs compared with untreated cells.

Concentration (µg/ml)	Mean activity ± SD	Sig	P Value
Untreated Cells	16216 ± 1149.63	0000	0000
100	32972 ± 2971.75	***	0.0006
200	48466±3580.018	****	<0.0001

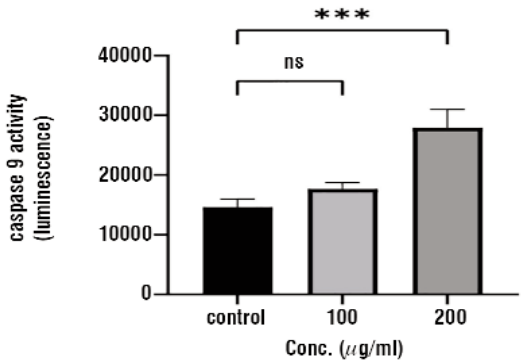


Figure 13 - Activation of caspase-9 activity by ZnO-NPs. Results were increase compared with untreated cell. Data represents mean ± SD of three independently repeated experiments

Table 6 - Comparison of caspase-9 activity in luminescence (Mean ± SD) in PC3 treated cells with 50, 100 and 200 µg/ml ZnO-NPs for 24 hours compared with untreated cells.

Concentration(µg/ml)	Mean activity ± SD	Sig	P Value
Untreated Cells	14664.33 ± 1306.5	0000	0000
100	17676.33 ± 1038.311	Ns	0.1945
200	27903 ± 3065.134	***	0.0004

DISCUSSION

Biosynthesis of Zinc Oxide Nanoparticles (ZnO-NPs)

Nanoparticles have gained significant attention due to their unique physicochemical properties, which enable them to conjugate with other functional groups owing to their charged surfaces (29). Among these, zinc oxide nanoparticles (ZnO-NPs) have attracted considerable interest in recent years due to their small size and high surface-to-volume ratio, making them ideal candidates for diverse applications, including biomedicine, electronics, and agriculture (30) The biosynthesis of ZnO-NPs using endophytic fungi has

emerged as a promising, eco-friendly, and cost-effective alternative to conventional physical and chemical synthesis methods (31). Several studies have reported the biosynthesis of ZnO-NPs using endophytic fungi, such as Fusarium oxysporum, Aspergillus fumigatus, and Trichoderma viride. In this process, metal ions are reduced to their corresponding nanoparticles, which are subsequently stabilized by various biomolecules, including proteins, polysaccharides, and enzymes secreted by the fungi (32). In the present study, ZnO-NPs were synthesized using the biomass of Aspergillus niger via an extracellular process. The formation of ZnO-NPs was confirmed by the appearance of a white precipitate at the end of the reaction. This phenomenon is attributed to the surface plasmon resonance (SPR) effect, following the reduction of Zn^{2+} ions from zinc sulfate in an aqueous medium. The fungal filtrate acts as both a reducing and a capping agent, facilitated by the presence of various extracellular proteins and enzymes (33,34).

Characterization of Synthesized Zinc Oxide Nanoparticles

The UV–Vis absorption spectrum provides critical insights into the electronic changes occurring in the produced nanoparticles. The detected absorption bands correspond to specific electronic transitions and can provide information about the nanoparticles' size, structure, and optical properties (35). This analysis showed an absorbance peak at 301 and 233, which was specific for the zinc oxide nanoparticles (36). The shift of the absorbance peak towards higher wavelengths indicate a transition from bulk materials to the nanoscale. This change is likely due to electron transitions, where an electron absorbs energy and moves from a lower energy state to a higher one (37). The diameter ranging of the spherical ZnO-NPS from 23.46 to 48.1 nm, the presence of larger particles may be result from unwanted aggregation occurring during the drying process. Agglomeration initiates as the liquid evaporates, resulting in an increased concentration of particles. The rising concentration of dissolved ions due to evaporation can reduced the electrostatic repulsive forces, thereby promoting agglomeration (38). The EDX analysis showed the presence of the expected constituent elements with minimal impurities, indicating the high purity of the sample and the effectiveness of the biological synthesis process. While AFM analysis revealed that the synthesized particles exhibited a uniform size distribution with an average size of approximately 73.99 nm. This indicates the efficiency of the synthesis method in controlling nanoparticle size and minimizing agglomeration. The results of EDX and AFM agreed with (39,40), respectively.

Cytotoxic Effects of the ZnO-NPs Using MTT Assay

Cancer is typically treated by conventional therapies such as chemotherapy, radiotherapy, and surgery. Although all these therapies are very effective in killing cancer cells, but they also result in many serious side effects. Recently, nanotechnology-based nanosystems, which exhibt biocompatibility, easy surface functionalization, cancer targeting and drug delivery capacity, have demonstrated the potential to overcome these side effects. ZnO NPs as nanomaterials can effectively improve the stability of clinical drugs and improve patients' drug absorption capacity. ZnO NPs have an important anticancer role in a variety of cancer types (41,42).

The anticancer effects of zinc oxide nanoparticles (ZnO-NPs) on cancer cells can be explained during several mechanism. One of the primary mechanisms is the increased accumulation of reactive oxygen species (ROS) within cancer cells, as demonstrated in various studies. ROS are highly reactive molecules that can induce oxidative stress, disrupt cellular processes, and ultimately result in DNA damage and cell death (43). Our cytotoxicity results are in agreement with recent studies showing that ZnO -NPs significantly induce cytotoxicity effects cancer cells while showing minimal effects on normal cells (44). For example, research has shown that ZnO-NPs exerted cytotoxic effects on several human glioma cell lines, including A172, U87, LNZ308, LN18, and LN229, (A172, U87, LNZ308 LN18, and LN229), and no cytotoxic effect was observed on normal human astrocytes. ZnO-NPs displayed a strong capacity to induce cell death in human myeloblastic leukemia cells (HL60) in comparison to normal peripheral blood mononuclear cells. (45).

Cytotoxic Effects of (ZnO-NPs) on PC-3 Cells Using HCS

High- content screening assay are powerful predictive assays for assessing morphological changes in cells resulting from toxic effects providing quantitative assessments of various parameters related to toxicity (46). Cell viability is an important toxicity assay parameter and is directly associated with the toxic effects of a drug (47). is a fundamental parameter in toxicity assay and is directly correlated with the

harmful effects of drugs. Research has shown that zinc oxide nanoparticles (ZnO-NPs) lead to a decrease in cell viability in PC-3 cells, with this reduction being influenced by both the concentration of ZnO -NPs and the density of the cells. Such effects may be due to cytostatic and cytotoxic mechanism that could potentially reduce telomerase activity (48).

The intensity of mitochondrial membrane permeability in PC-3 cells increases with higher concentration of ZnO-NPs, a result of necrosis or apoptosis, which disrupt mitochondria function. These changes can lead to a loss of mitochondrial membrane potential and the release of cytochrome c from the mitochondria. (49). Changes in cell membrane permeability are often associated with a toxic or apoptotic response and cytotoxicity can damage membrane integrity (50). ZnO-NPs can alter the lipid composition and structural arrangement within both intracellular and plasma membranes, resulting in changes to plasma membrane permeability during the activation of second messenger pathway via the phospholipase pathway and sustained protein kinase C activation. This increased membrane permeability, along with extended protein kinase C activity, can also affect the binding of rod outer segments (51).

Mitochondrial membrane potential is a crucial indicator of functional mitochondria and treatment with ZnO- NPs at different concentrations reduces this potential in PC-3 cells in a dose-dependent manner. It was suggested that ZnO-NPs may disrupt the permeability transition pores of mitochondrial membrane, allowing the transition of molecules and ions that interrupts the respiratory chain, facilitates the release of cytochrome C and triggering apoptosis (52).

Caspase-8 and Caspase-9 Induction

The discovery of novel and effective antitumor drug that specifically target tumor cells by activation of apoptosis become a vital concern in cancer treatment (53). The molecular mechanism of ZnO-NPs contains apoptosis during the activation of effector caspase-8 and 9 was investigated. The treatment of PC-3 cells with ZnONPs significantly stimulated the cleavage of caspases- 8 and 9 precursors in dose dependent pattern, resulting in increased activation of both enzyme and thus induced intrinsic and extrinsic pathway of cell apoptosis.

The increased level of caspase 8 strongly indicate that treatment with ZnO-NPs activates this caspase. The activation of caspase-8 is directly associates to series of cellular event leads to apoptosis, starting with the truncation of the Bid protein by caspase-8 into its active pro apoptotic form (tBid) which connects the receptors mediated activation of caspase-8 to mitochondrial cell death events (54,55). Additionally, the activation of caspase-9 by ZnO-NPs, suggests that likely mediate the mitochondrial cell death pathway in PC-3 cell confirmed by the observation of mitochondrial membrane disruption, cytochrome C release into the cytoplasm and subsequent elevation in caspase-9 level Moreover, ZnO-NPs considered as natural inhibitor of 5-lipoxygenase, a proinflammatory enzyme that catalyzes the biosynthesis of leukotrienes that accountable for many diseases (56).

CONCLUSION

The A. niger extract-derived ZnO nanoparticles (ZnO-NPs) were studied for their anticancer properties. The high cost and adverse side effects associated with conventional chemotherapeutic agents have necessitated the exploration of natural products as potential alternatives or adjuvants to conventional anticancer drug. The results demonstrated that zinc oxide nanoparticles (ZnO-NPs) of A. niger extract promising anticancer properties. However, further research is needed to determine the precise mechanism of action against the prostate cancer, so that this novel (ZnO-NPs) formulation can be verified in a specific in vivo model and further utilized for the good of global society.

Conflicts of Interest

Authors declared no any conflict.

REFERENCES

1. Sung H, Ferlay J, Siegel RL, Laversanne M, Soerjomataram I, Jemal A, et al. Global cancer statistics 2020: GLOBOCAN estimates of incidence and mortality worldwide for 36 cancers in 185 countries. CA Cancer J Clin. 2021;71(3):209–249.
2. Al-Mugdadi SFH. Diagnostic biomarkers related to cancer detection and treatment: A review article. Univ Thi-Qar J Sci. 2021;8:3–6.
3. Banerjee PP, Banerjee S, Brown TR, Zirkin BR. Androgen action in prostate function and disease. Am J Clin Exp Urol. 2018;6(2):62–77.
4. Siegel RL, Miller KD, Jemal A. Cancer statistics, 2020. CA Cancer J Clin. 2020;70(1):7–30.
5. Miller KD, Siegel RL, Lin CC, Mariotto AB, Kramer JL, Rowland JH, et al. Cancer treatment and survivorship statistics, 2016. CA Cancer J Clin. 2016;66(4):271–289.
6. Cheng Z, Li M, Dey R, Chen Y. Nanomaterials for cancer therapy: Current progress and perspectives. J Hematol Oncol. 2021;14:85.
7. Jabir NR, Tabrez S, Ashraf GM, Shakil S, Damanhouri GA, Kamal MA. Nanotechnology-based approaches in anticancer research. Int J Nanomedicine. 2012;7:4391–4408.
8. Wu J, Wang Y, Yang X, Liu Y, Yang J. Nanotechnology in cancer diagnosis and therapy. Nanotechnology. 2012;23:1-5.
9. Faisal S, Al-Radadi NS, Jan H, Abdullah SA, Shah S, Bibi N. Curcuma

longa mediated synthesis of copper oxide, nickel oxide and Cu-Ni bimetallic hybrid nanoparticles: Characterization and evaluation for antimicrobial, anti-parasitic and cytotoxic potentials. Coatings. 2021; 11(7):849.
10. Al-Radadi NS, Hussain T, Faisal S, Shah AAR. Novel biosynthesis, characterization and bio-catalytic potential of green algae (Spirogyra hyalina) mediated silver nanomaterials. Saudi J Biol Sci. 2022; 29(1):411–419.
11. Ullah R, Shah S, Muhammad Z, Shah SA, Faisal S, Khattak U, et al. In vitro and in vivo applications of Euphorbia wallichii shoot extract-mediated gold nanospheres. Green Process Synth. 2021;10(1):101–111.
12. Sedefoglu N, Zalaoglu Y, Bozok F. Green synthesized ZnO nanoparticles using Ganoderma lucidum: Characterization and in vitro nanofertilizer effects. J Alloys Compd. 2022;918:165695.
13. Yusof HM, Mohamad R, Zaidan UH, Rahman NAA. Sustainable microbial cell nanofactory for zinc oxide nanoparticles production by zinc-tolerant probiotic Lactobacillus plantarum strain TA4. Microb Cell Fact. 2020;19:10.
14. Bhardwaj K, Sharma A, Tejwan N, Bhardwaj S, Nepovimova E, Kuca K. Pleurotus macrofungi-assisted nanoparticle synthesis and its potential applications: A review. J Fungi (Basel). 2020;6(4):351.
15. Kalpana VN, Kataru BAS, Sravani N, Vigneshwari T, Panneerselvam A, Rajeswari VD. Biosynthesis of zinc oxide nanoparticles using culture filtrates of Aspergillus niger: Antimicrobial textiles and dye degradation studies. OpenNano. 2018;3:48–55.
16. Al-Radadi NS, Faisal S, Alotaibi A, Ullah R, Hussain T, Rizwan M, et al. Zingiber officinale driven bioproduction of ZnO nanoparticles and their anti-inflammatory, anti-diabetic, anti-Alzheimer, anti-oxidant, and anti-microbial applications. Inorg Chem Commun. 2022; 140:109274.
17. Riyadh S, Mohammad MS, Naser NR. Optical properties of germanium nanoparticles prepared by laser ablation. Univ Thi-Qar J Sci. 2023;10:137–140.
18. Aqab TBM. The biological effect of melanin pigment extracted from Aspergillus niger and possibility of its use in improving the qualitative of laboratory biscuit [master's thesis]. Baghdad (Iraq): University of Baghdad, College of Education for Women; 2023.
19. Balsam MM. Myco-biosynthesis of silver nanoparticles by Aspergillus niger and evaluation of their antifungal activity in Dermatophytes spp. and Candida albicans [PhD dissertation]. Al-Qadisiyah (Iraq): College of Medicine, University of Al-Qadisiyah; 2017.
20. Elumalai K, Velmurugan S, Ravi S, Kathiravan V, Ashokkumar S. Green synthesis of zinc oxide nanoparticles using Moringa oleifera leaf extract and evaluation of its antimicrobial activity. Spectrochim Acta A Mol Biomol Spectrosc. 2015;143:158–164.
21. El-Megharbel SM, Refat MS, Al-Salmi FA, Hamza RZ. In situ neutral system synthesis, spectroscopic, and biological interpretations of magnesium(II), calcium(II), chromium(III), zinc(II), copper(II), and selenium(IV) sitagliptin complexes. Int J Environ Res Public Health. 2021;18(15):8030.
22. Bhattacharyya P, Agarwal B, Goswami M, Maiti D, Baruah S, Tribedi P. Zinc oxide nanoparticle inhibits the biofilm formation of Streptococcus pneumoniae. Antonie Van Leeuwenhoek. 2018; 111(1):89–99.
23. Ali HH. Preparation and characterization of ZnO NWs/graphene nanocomposite as an effective photoanode electrode for improving the performance of dye-sensitized solar cells. Univ Thi-Qar J Sci. 2023;10:11-15.
24. Du WL, Xu ZR, Han XY, Xu YL, Miao ZG. Preparation, characterization and adsorption properties of chitosan nanoparticles for eosin Y as a model anionic dye. J Hazard Mater. 2008;153(1–2):152–156.
25. Hodoroaba VD. Energy-dispersive X-ray spectroscopy (EDS). In: Hodoroaba VD, Unger WES, Shard AG, editors. Characterization of Nanoparticles: Measurement Processes for Nanoparticles. Amsterdam: Elsevier; 2019. p. 397–448.
26. Rashid H, Umamaheswari G. Evaluation of the cytotoxic effect of ginger extract against prostate cancer model using in vitro study. World J Pharm Pharm Sci. 2017;6(12):1044–1053.
27. Ali Z, Al-Saffar FA, Sabry SL, Al-Brazanchi AF, Al-Shanon FH, Hadi NA. Phytochemical analysis, antioxidant and cytotoxic potentials of Pelargonium graveolens extract in human breast adenocarcinoma (MCF-7) cell line. Asian J Biochem. 2017;12:16–26.
28. Looi CY, Arya A, Cheah FK, Muharram B, Leong KH, Mohamad K, et al. Induction of apoptosis in human breast cancer cells via caspase pathway by vernodalin isolated from Centratherum anthelminticum (L.) seeds. PLoS One. 2013;8(2):e56643.
29. Chavan RR, Bhinge SD, Bhutkar MA, Randive DS, Wadkar GH, Todkar SS, et al. Characterization, antioxidant, antimicrobial and cytotoxic activities of green synthesized silver and iron nanoparticles using alcoholic Blumea eriantha DC plant extract. Mater Today Commun. 2020;24:101320.
30. Gomaa EZ. Microbial mediated synthesis of zinc oxide nanoparticles, characterization and multifaceted applications. J Inorg Organomet Polym Mater. 2022;32(11):4114–4132.
31. Mohd Yusof H, Mohamad R, Zaidan UH, Abdul Rahman NA. Microbial synthesis of zinc oxide nanoparticles and their potential application as an antimicrobial agent and a feed supplement in animal industry: A review. J Anim Sci Biotechnol. 2019;10:57.
32. Bachheti RK, Abate L, Bachheti A, Madhusudhan A, Husen A. Algae, fungi-, and yeast-mediated biological synthesis of nanoparticles and their various biomedical applications. In: Husen A, Iqbal M, editors. Handbook of Greener Synthesis of Nanomaterials and Compounds. Elsevier; 2021. p. 701–734.
33. Mekky AE, Farrag AA, Hmed AA, Sofy AR. Preparation of zinc oxide nanoparticles using Aspergillus niger as antimicrobial and anticancer agents. J Pure Appl Microbiol. 2021;15(3):1547–1566.
34. Rajan A, Cherian E, Baskar G. Biosynthesis of zinc oxide nanoparticles using Aspergillus fumigatus JCF and its antibacterial activity. Int J Mod Sci Technol. 2016;1(2):52–57.
35. Hameed H, Waheed A, Sharif MS, Saleem M, Afreen A, Tariq M, et al. Green synthesis of zinc oxide (ZnO) nanoparticles from green algae and their assessment in various biological applications. Micromachines. 2023;14(5):928.
36. Aral K, Aral CA, Kapila Y. The role of caspase-8, caspase-9 and apoptosis-inducing factor in periodontal disease. J Periodontol. 2019;90(3):288–294.
37. Jain N, Bhargava A, Tarafdar JC, Singh SK, Panwar J. A biomimetic approach towards synthesis of zinc oxide nanoparticles. Appl Microbiol Biotechnol. 2013;97(2):859–869.
38. Abdullah SM, Al-Hamdani AA, Al-Zubaidi LA. Water treatment using zinc nanoparticles and apricot plant extracts from organic and inorganic pollution. Baghdad Sci J. 2024;21(1):124–124.
39. Alamdari S, Sasani Ghamsari M, Lee C, Han W, Park HH, Tafreshi MJ, et al. Preparation and characterization of zinc oxide nanoparticles using leaf extract of Sambucus ebulus. Appl Sci. 2020; 10(10):3620.
40. Al-Janabi TYS. Biosynthesis of zinc oxide nanoparticles by Pseudomonas aeruginosa locally isolated [thesis]. Baghdad (Iraq): University of Baghdad, College of Education for Pure Sciences/Ibn Al-Haitham; 2019.
41. Gu W, Yang C. Zinc oxide nanoparticles inhibit malignant progression and chemotherapy resistance of ovarian cancer cells by activating endoplasmic reticulum stress and promoting autophagy. Exp Ther Med. 2023;26(5):508.
42. Perumal P, Sathakkathulla NA, Kumaran K, Ravikumar R, Selvaraj JJ, Nagendran V, et al. Green synthesis of zinc oxide nanoparticles using aqueous extract of shilajit and their anticancer activity against HeLa cells. Sci Rep. 2024;14(1):2204.
43. Zahin N, Anwar R, Tewari D, Kabir MT, Sajid A, Mathew B, et al. Nanoparticles and its biomedical applications in health and diseases: Special focus on drug delivery. Environ Sci Pollut Res Int. 2020; 27(16):19151–19168.
44. Ostrovsky S, Kazimirsky G, Gedanken A, Brodie C. Selective cytotoxic effect of ZnO nanoparticles on glioma cells. Nano Res. 2009;2:882–890.
45. Premanathan M, Karthikeyan K, Jeyasubramanian K, Manivannan G. Selective toxicity of ZnO nanoparticles toward Gram-positive bacteria and cancer cells by apoptosis through lipid peroxidation. Nanomedicine. 2011;7(2):184–192.

46. Al-Dulimi AG, Al-Saffar AZ, Sulaiman GM, Khalil KA, Khashan KS, Al-Shmgani HS, et al. Immobilization of L-asparaginase on gold nanoparticles for novel drug delivery approach as anticancer agent against human breast carcinoma cells. J Mater Res Technol. 2020;9:15394–15411.
47. Al-Jailawi MH, Nasir HM, Aziz GM. Cytotoxic effect of biosurfactants produced by novel thermophilic Geobacillus thermoleovorans (JQ912239). Int J Adv Res. 2015;3:632–637.
48. Ajabnoor GM, Crook T, Coley HM. Paclitaxel resistance is associated with switch from apoptotic to autophagic cell death in MCF-7 breast cancer cells. Cell Death Dis. 2012;3:e260.
49. Hassan F, Mohammed G, El-Hiti GA, Alshanon A, Yousif E. Cytotoxic effects of tamoxifen in breast cancer cells. J Unexplored Med Data. 2018;3(3):1–10.
50. Al-Saily HM, Al-Halbosiy MM, Al-Hady FN. Cytotoxic and apoptotic effects of cyproterone acetate against cancer cells and normal cells. J Biotechnol Res Center. 2019;13:68–74.
51. Khadka NK, Cheng X, Ho CS, Katsaras J, Pan J. Interactions of the anticancer drug tamoxifen with lipid membranes. Biophys J. 2015;108(10):2492–2501.
52. Li H, Li X, Bai M, Suo Y, Zhang G, Cao X. Matrine inhibited proliferation and increased apoptosis in human breast cancer MCF-7 cells via upregulation of Bax and downregulation of Bcl-2. Int J Clin Exp Pathol. 2015;8:14793–14799.
53. Pistritto G, Trisciuoglio D, Ceci C, Garufi A, D'Orazi G. Apoptosis as anticancer mechanism: Function and dysfunction of its modulators and targeted therapeutic strategies. Aging (Albany NY). 2016; 8(4):603–619.
54. Kim WS, Lee KS, Kim JH, Kim C, Lee G, Choe J, et al. The caspase-8/Bid/cytochrome c axis links signals from death receptors to mitochondrial reactive oxygen species production. Free Radic Biol Med. 2017;112:567–577.
55. Schug ZT, Gonzalvez F, Houtkooper RH, Vaz FM, Gottlieb E. BID is cleaved by caspase-8 within a native complex on the mitochondrial membrane. Cell Death Differ. 2011;18:538–548.
56. Bolbolian S, Bozorgmehr MR, Morsali A. Acetyl-11-keto-β-boswellic acid derivatives effects on 5-lipoxygenase: In silico viewpoint. J Mol Graph Model. 2020;94:107464.